ISSN 1846-6168 (Print), ISSN 1848-5588 (Online)
https://doi.org/10.31803/tg-20220329131808

Original scientific paper
Received: 2022-03-29, Accepted: 2022-04-11

Performance Optimisation of Single-Phase Variable Reluctance Shaded-Pole Motor

Adem Dalcalı*, Mehmet Akbaba

Abstract: Shaded pole induction motors' theoretical analysis is quite difficult because of the presence of strong harmonic components and the elliptical rotating field. The change of air gap reluctance is affecting the air gap flux distribution and thus the performance of the motor. In the study, the effect of the change in the SPIM's stator, rotor and squirrel cage on the performance of the motor is analysed by the Finite Element Method. The flux distributions and torque values of the closed-interpoles type and the stator with different interpoles clearances are obtained. The effects of single and double cage structures in the rotor part and the effects of copper and aluminium cage materials in the squirrel cage were analysed. According to the analyses, it was determined that the single cage motor with aluminium cage material exhibited the best torque performance with a torque value of 132.78 mNm.

Keywords: double cage; elliptical rotating field; finite element method; shaded-pole motor; single cage

1 INTRODUCTION

When voltage is applied to the stator of three-phase induction motors, a rotating field is produced, and the motor starts to rotate. The resulting rotating field circulates current in the rotor, which creates a closed circuit. The interaction between the field formed by these currents and the rotating field of the stator ensures the rotation of the rotor. In three-phase induction machines, the placement of the windings with a 120˚ phase difference provides the formation of the rotating field. However, in single-phase induction machines, the rotating field cannot be created since a single phase is applied to the stator. Therefore, the machine should be manufactured with auxiliary winding or shaded pole to prevent this situation in single-phase induction motors [1-3]. Shaded pole induction motors are preferred, especially in low-power applications, due to their simple structure, low cost, and direct operation from a single-phase source [4, 5]. However, these motors cannot compete with three-phase motors, especially in industrial applications that require high power.

Although Shaded pole induction motors (SPIMs) are structurally simple, they are among the electrical machines that are theoretically the most difficult to analyse. This difficulty is due to the fact that SPIMs have an elliptical rotating magnetic field. When studies in the literature was reviewed, it was observed they focused on the finite element analysis (FEA) of the shaded pole motors. Four different motor models were designed, and 2D FEAs were performed under different load conditions. The magnetic flux density and saturation regions in the core were determined by performing the magnetostatic and transient analyses of the models [6]. In another analysis study, the skew effect of the rotor bars was realized by creating n-piece structures. The authors preferred the 2D analysis method since 3D analyses would cause longer analysis time [7]. Unlike this study, Shamlou and Mirsalim preferred 3D analyses since short-circuit resistance, winding leakage inductance, and skew cannot be directly taken into account in 2D analyses [8]. When the performance improvement studies of the SPIM were reviewed, it was observed that the effects of structural and different materials on the shaded pole ring, stator, and rotor were investigated. In the study investigating the effect of the short-circuit ring on the motor, it was determined that the reverse rotating magnetic field component was less in the double short circuit ring motor, which resulted in the reduction of vibrations in the torque characteristic [9]. The dynamic model of the shaded pole motor can be derived using the step response of the circuit approach. With this method, the effect of core losses, which is generally neglected, can also be added to the model [10]. Another analysis method is the symmetrical components theory. In this method, the accuracy of the results depends on taking the parameters right and complete [11]. In the analysis of the shaded pole motor performed using the symmetrical components theory, high order harmonic components were neglected in the study conducted by considering only the fundamental harmonics. However, the fact that the SPIM has high harmonic components reduces the accuracy of the study in this sense [11]. The design problem of SPIMs can be considered a vector optimization problem. Aluzri used the problem in the analysis of the cost of the motor and the starting torque using a nonlinear programming technique [12].

Finite element analyses are used in the approximate analysis of the quantities which are used in the analysis of electrical machines and are continuous in a certain region such as electric and magnetic fields. In this method, these continuous quantities are divided into a finite number of small regions that can be expressed by partial differential equations. To obtain the solution at a point in the region, the contribution of the elements surrounding that point is taken into account. Thus, a set of linear equations with as many equations as the number of nodes is derived, and the desired quantities are calculated. Performance and design criteria such as core losses and flux distributions of the machine can be obtained by analyses [13-15]. In the SPIM, starting torques are small compared to other single-phase motors with auxiliary winding. SPIMs are low-efficiency motors, although they are widely used [16]. Starting torques can be developed using structural designs and developing material technology.

In this study, analysis of a variable reluctance shaded pole induction motor is carried out using the finite element method. The effects of closed-interpoles (i.e. without clearance between the stator interpoles) type structure and different aperture stator on motor performance are investigated. In addition, the effect of squirrel cage material on the performance is also investigated. The paper has been structured as follows: In section II the operating principle of the shaded pole motors and the characteristics of the motor under investigation subject to study is given. In section III, the torque and magnetic flux distributions of different structures of the motor are investigated. Section 4 draws conclusions.

2 SHADED POLE MOTORS IN GENERAL AND THE PROPOSED MOTOR

While the rotor of SPIMs is squirrel-cage, the stator consists of salient poles. A field is formed as a result of a single-phase alternating voltage applied to the main winding in the salient poles. This field also induces a field in the rotor. However, torque cannot be generated in the motor. There is a need for shaded poles so that the motor can generate torque. Copper rings serve to provide starting. The voltage induced in the shaded pole due to the main winding causes short-circuit currents to flow in the short-circuited slit pole rings. These currents create a flux in the almost backward phase compared to the stator flux. These two alternative fields allow the motor to run by creating an elliptical rotating field in the air gap. The rotor moves from the non-shaded pole part of the stator pole to the shaded pole part of it with the effect of the elliptical rotating field given in Eq. (1). The field created by the pole winding slips toward the commutating field. When the current changes direction, this time the polarity of the poles changes, and again the slip direction of the field remains the same [1].

$$\Phi_s = \Phi_a + \Phi_{sp} \tag{1}$$

The relative states of the stator winding area and slit pole ring areas, and flux phasor diagrams are presented in Fig. 1.

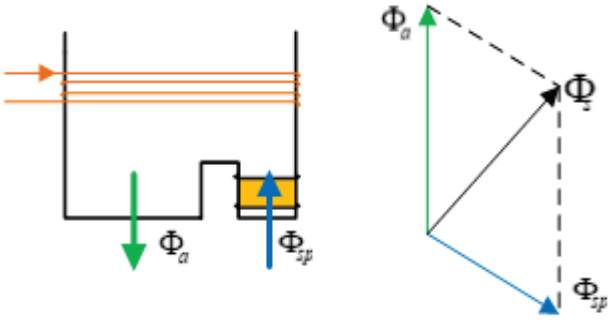

Figure 1 Flux paths and flux diagram of the SPIM

Shaded pole induction motors with variable air gap are electrical machines that are easy to manufacture but difficult to analyse mathematically. The first reason for the simplicity in their structure is that the auxiliary winding consists of copper rings placed in the slits opened on the stator poles. The second reason is that the stator windings are collectively placed on salient poles. The reasons for the difficulty of the mathematical analysis are the presence of harmonic components in the stator magnetomotive force and the ellipticity of the rotating field [17]. The comparison of single-phase induction motors is summarily presented in Tab. 1 [18, 19]

Table 1 Characteristics of single-phase induction motors

Motor Type	Power (HP)	Efficiency (%)	Application Area
Auxiliary winding	1/20 - 1	55-65	Aspirator, dishwasher etc. That require low starting torque applications
Capacitor-start	0.125 - 1	55-65	Compressor, refrigerator, washing machine, pump
Permanent split capacitor	0.125 - 1	60-70	Low noise applications such as aspirator, pump
Shaded pole	1/200 - 1/20	25-40	Applications requiring low starting torque such as aspirator, hair dryer

The initial model of the motor discussed in the study is presented in Fig. 2 [20].

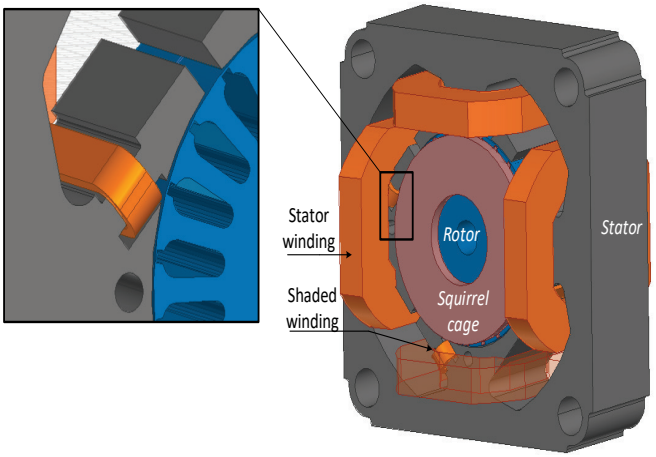

Figure 2 SPIM model

The dimensions and characteristics of the motor used in the study are presented in Tab. 2.

Table 2 Motor characteristics

Property	Value
Voltage (V)	220
Number of poles	4
Number of slot	26
Core size (mm)	82×82×25
Number of winding turns	580
Stator core material	M43
Rotor core material	Stell-1010
Rotor type	Squirrel cage
Power (W)	15

3 PERFORMANCE EVALUATION

The design of electrical machines requires the solution of interrelated problems of electromagnetic, mechanical,

thermal, and material technology. The designer determines input variables and constraints by considering the cost and desired performance criteria. The design of the machine that exhibits the expected characteristics requires long-term analysis and investigation. The performance of the machine is affected by many physical parameters such as the number of stator slots, the number of rotor slots, and the slot structure of the machine [21]. In this section, three different structures of the stator are first examined. In the first case, the closed-interpoles stator structure (Fig. 3a) is investigated. In the second case, the stator interpoles clearance is selected as 4 mm (Fig. 3b), and in the last case, the stator interpoles clearance is selected as 8 mm (Fig. 3c).

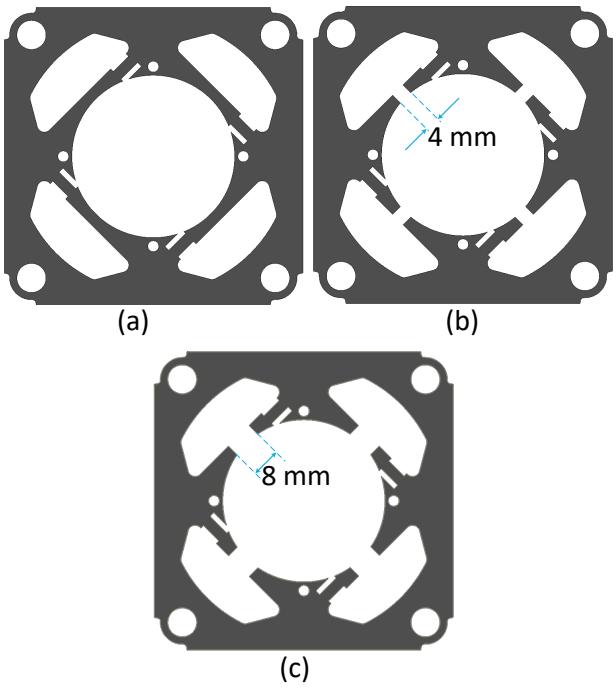

Figure 3 Stator geometry

Except for the specified clearance, the stator parameters were left constant. Thus, only the effect of this parameter are examined. It is important to know the distribution of the magnetic field in the motor in the design and determination of the operating characteristics of the SPIM. The net flux of a closed surface in a magnetic field can be written as follows [22];

$$\int_s \vec{B}\,\mathrm{d}s = 0 \tag{2}$$

The linear integral of the magnetic field along a closed circumference in a magnetic field is equal to the sum of the currents enclosed by the circumference and is expressed by Eq. (3).

$$\int \vec{H}\,l = \sum I \tag{3}$$

By expressing the surface of the closed circumference as s, assuming that the current is uniformly distributed over the surface with a constant current density (J);

$$\int_c \vec{H}\,\mathrm{d}l = \int_s \vec{J}\,\mathrm{d}s \tag{4}$$

can be written. According to the Stokes theorem.

$$\int_s rot\,\vec{H}\,\mathrm{d}s = \int_s \vec{J}\,\mathrm{d}s \tag{5}$$

and

$$rot\,\vec{H} = \vec{J} \tag{6}$$

are obtained. If Eq. (6) is rewritten with the $\vec{B} = \mu\vec{H}$ relation between the magnetic field strength and magnetic flux density.

$$rot\left(\frac{1}{\mu}\vec{B}\right) = \vec{J} \tag{7}$$

The magnetic field can be derived from a vector function, which we will denote by $\vec{A}$.

$$\vec{B} = rot\,\vec{A} \tag{8}$$

If Eq. (7) is arranged with the help of Eq. (8) by using $1/\mu = v$.

$$rot\,(v\,rot\,\vec{A}) = \vec{J} \tag{9}$$

is obtained.

$$rot(\vec{A}) = \begin{bmatrix} \frac{\partial}{\partial x} & \frac{\partial}{\partial y} & \frac{\partial}{\partial z} \\ 0 & 0 & A \end{bmatrix} = \frac{\partial A}{\partial y}\vec{i} - \frac{\partial A}{\partial x}\vec{j} \tag{10}$$

If Eq. (10) is combined with the relation $rot\,(vrot\vec{A}) = \vec{J}$.

$$\frac{\partial}{\partial x}\left(v\frac{\partial A}{\partial x}\right) + \frac{\partial}{\partial y}\left(v\frac{\partial A}{\partial y}\right) = -\vec{J} \tag{11}$$

The solution of the magnetic field distribution in the motor is obtained from the solution of Eq. (11) by FEA. The flux density distribution in the case of the main winding and squirrel cage excitation is obtained in 3 different structures and are presented in Fig. 4.

When the flux distributions are examined, especially in case of closed-interpoles stator structure, a large amount of flux completes its circuit over the stator instead of passing through the high reluctance air gap to the rotor. In this case, it creates a high flux density in the relevant parts. When

rotors are analysed, less flux density is observed in the closed-interpoles structure compared to other structures due to less flux passing to the rotor. It is observed that useful common flux is higher in open-interpoles structures, which is the first indication that it will result in outstanding performance.

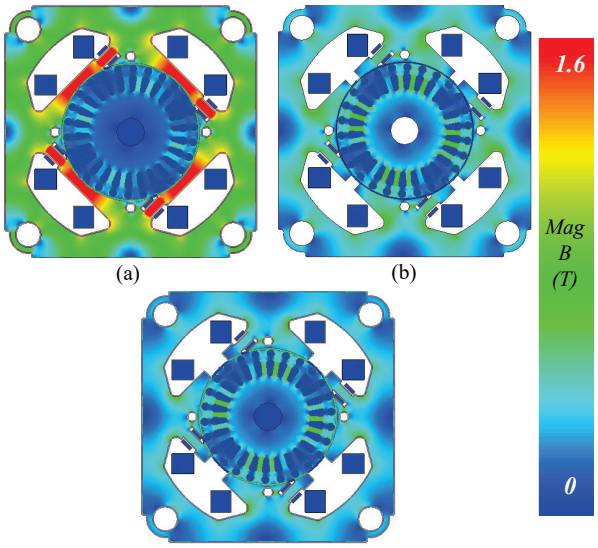

Figure 4 Magnetic flux density distribution; a) closed-interpoles, b) clearance 4 mm, c) clearance 8 mm (both main winding and squirrel cage excited)

The flux density distribution performed only in the main winding excited state was obtained in 3 different structures and is presented in Fig. 5.

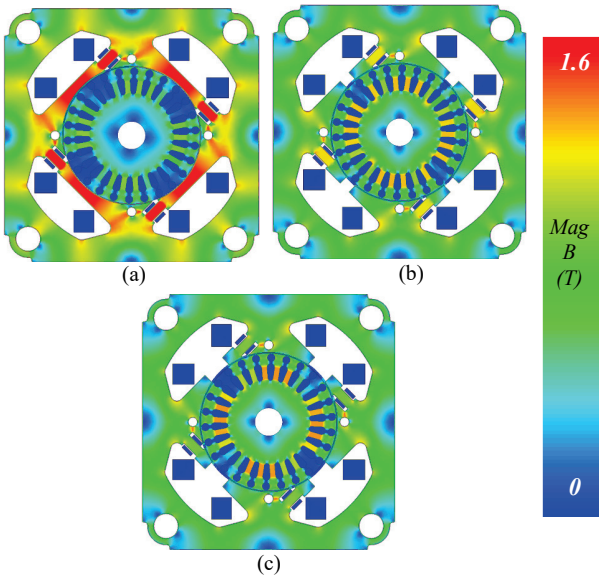

Figure 5 Magnetic flux density distribution; a) closed-interpoles, b) clearance 4 mm, c) clearance 8 mm (only with main winding excited)

3.1 Comparison of Single and Double Cage Rotor Designs

In this section, a squirrel cage rotor is designed as a single and double cage, and their performances are examined. Copper was used as the squirrel cage material. The structures used in the study and their dimensions are presented in Fig. 6.

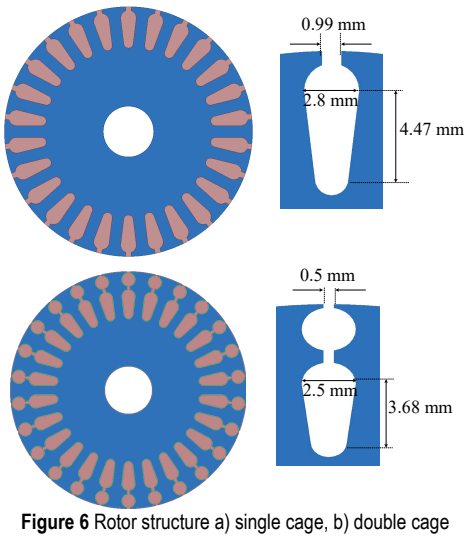

Figure 6 Rotor structure a) single cage, b) double cage

The torque values obtained in analyses performed when the slip value was 0.1 are presented in Tab. 3. Copper was preferred in the squirrel cage material in the analyses.

Table 3 Induced torque values

Slip	Rotor type	0 (closed type)	4 mm	8 mm
$s = 0.1$	Single	84.87 mNm	111.51 mNm	97.46 mNm
	Double	55.16 mNm	85.74 mNm	81.02 mNm

The torque values of the double cage structure are found to be relatively higher. Furthermore, less useful flux transferred to the rotor in the closed-type stator caused the induced torque to be low in this structure. It is observed that torque value is maximum in the structure with a 4 mm interpoles-clearances. Flux distributions in single and double cage rotors are presented in Fig. 7. Appropriate flux distributions are obtained for the slots in the designs. However, the designer should consider the flux density in the selection of the number of slots so that the teeth are not saturated, especially in high numbers of slots.

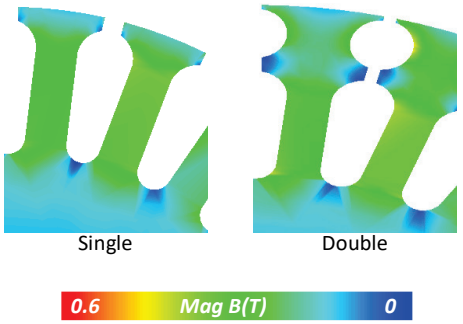

Figure 7 Flux density distribution

3.2 Comparison of Copper and Aluminium Rotor Conductors

The material of the cage is another parameter that can be examined in squirrel cage motors. In this study, as squirrel cage material copper and aluminium are used and resulting

performance are analysed separately. The conductivity of copper is better by 60% compared to aluminium material. However, the high melting point and the high cost of the copper at the production stage constitute a disadvantage [23]. The torque values obtained in analyses when the slip value is 0.1 are presented in Tab. 4. In the analyses, the rotor structure was chosen as a double cage.

Table 4 Induced torque values

Slip	Cage type	0 (closed-interpoles type)	4 mm	8 mm
$s = 0.1$	Copper	55.16 mNm	85.74 mNm	81.02 mNm
	Aluminium	66.18 mNm	99.17 mNm	96.05 mNm

The aluminium cage motor provided higher torque in all three structures compared to the copper cage motor. However, the fact that the resistance of aluminium is higher compared to copper causes high rotor Joule loss. The higher Joule loss will also result in lower efficiency in an aluminium motor compared to a copper motor. Finally, in the analysis of the single cage and aluminium structure, motor, the highest torque rating of 132.78 mNm has been obtained.

4 CONCLUSION

SPIMs are frequently preferred in the industry due to their low cost and simple structure, especially in low-power applications. In this respect, it is important to improve the performance of these low-efficiency machines. In this study, magnetostatic and transient analyses of the variable reluctance SPIM were performed, and magnetic flux distributions and induced torque values are analysed. The stator body is designed in three different structures, and the flux distributions in the core are derived. The flux distributions are derived for the cases when only the main winding is excited and when both the main winding and squirrel cage are excited. Especially in the closed-interpoles structure, the a large portion of the useful flux completes its circuit over the stator instead of passing to the rotor, which resulted in low induced torque and high flux density, which means high saturation and high iron losses, in the closed-interpole areas. In this type of structures, designers should pay attention to the saturation, especially in the bridge parts. In the analyses performed on the rotor part, single and double cage structures are examined. In the single cage structure, the torque value of 111.51 mNm was obtained at the highest value in the structure with a clearance of 4 mm. After this analysis, the material of the cage was changed to aluminium and the induced torques are obtained. Higher torque is obtained in the aluminium cage motor compared to the copper motor. Investigations showed that a highest torque of 132.78 mNm is obtained in the case of single cage rotor with aluminium bars and end rings.

Notice

The paper was presented at the International Congress of Electrical and Computer Engineering (ICECENG'22), which took place in Bandırma (Turkey), on February 9-12, 2022. The paper will not be published anywhere else.

5 REFERENCES

[1] Kurita, N., Ishikawa, T., & Suzuki, G. (2016). Development of the two pole type shaded pole self-bearing motor. *Materials Science Forum, 856*, 196-201. https://doi.org/10.4028/www.scientific.net/MSF.856.196

[2] Enesi, Y. A., Tsado, J., Nwohu, M., Usman, U. A., & Imoru, O. A. (2016). Split-phase motor running as capacitor starts motor and as capacitor run motor. *Leonardo Electronic Journal of Practices and Technologies, 15*(28), 253-272.

[3] Crăciunescu, A. (2019). The Development of a New Type of Repulsion-Induction Motor. *2019 IEEE International Electric Machines & Drives Conference (IEMDC)*, 1447-1451. https://doi.org/10.1109/IEMDC.2019.8785265

[4] Nakuã, L. & Spahiu, A. (2018). Saving energy by replacing IM with BLDC MOTOR in fan application. *European Journal of Electrical Engineering and Computer Science, 2*(5). https://doi.org/10.24018/ejece.2018.2.5.27

[5] Alidousti, A., Sadoughi, A., Behbahanifard, H., & Raeisi, Y. (2018). A new rotor prototype for single phase line start permanent magnet synchronous motor based on amendments to a small industrial shaded pole induction motor. *The 9th Annual Power Electronics, Drives Systems and Technologies Conference (PEDSTC)*, 218-223. https://doi.org/10.1109/PEDSTC.2018.8343799

[6] Sarac, V. & Cundev, D. (2012). Electromagnetic fields calculation at single phase shaded pole motor. *Electrotechnica & Electronica, 47*(7-8/20), 41-45.

[7] Petkovska, L., Cundev, M., & Sarac, V. (2002). FEM analysis of asymmetrical magnetic field in electrical machines. *The 2nd International Conference on Advanced Computational Methods in Engineering*, 1-10.

[8] Shamlou, S. & Mirsalim, M. (2015, November). A new restructured shaded pole induction motor-3D finite element analysis and experimental verification. *The 30th International Power System Conference (PSC)*, 136-141. https://doi.org/10.1109/IPSC.2015.7827739

[9] Pessina, G. & Morra, E. (2010, June). Optimization and design of the shaded pole single phase asynchronous motor. *SPEEDAM 2010*, 978-981. https://doi.org/10.1109/SPEEDAM.2010.5544905

[10] Ojaghi, M. & Daliri, S. (2015, October). A detailed dynamic model for single-phase shaded pole induction motors. *The 18th International Conference on Electrical Machines and Systems (ICEMS)*, 1987-1992. https://doi.org/10.1109/ICEMS.2015.7385366

[11] Sarac, V., Petkovska, L., & Cundev, M. (2001). An improved performance analysis of a shaded pole motor. *Proceedings of the Power Electronics Intelligent Motion and Power Quality Conference*, 399-405.

[12] Aluzri, A. M. & Mohammed, I. A. (2002). Vector optimization design of a shaded-pole induction motor. *IEEE Transactions on Energy Conversion, 17*(3), 374-379. https://doi.org/10.1109/TEC.2002.801990

[13] Dalcalı, A. & Akbaba, M. (2017). Comparison of the performance of bridge and bridgeless shaded pole induction motors using FEM. *International Journal of Applied Electromagnetics and Mechanics, 54*(3), 341-350. https://doi.org/10.3233/JAE-160133

[14] Dalcali, A. & Akbaba, M. (2016). Comparison of 2D and 3D magnetic field analysis of single-phase shaded pole induction

motors. *Engineering Science and Technology, an International Journal, 19*(1), 1-7. https://doi.org/10.1016/j.jestch.2015.04.013
[15] Çetin, O., Dalcalı, A., & Temurtaş, F. (2020). Estimation of Permanent Magnet Synchronous Generator Performance with Artificial Neural Network Models. *Sakarya University Journal of Computer and Information Sciences, 3*(1), 60-73. https://doi.org/10.35377/saucis.03.01.724976
[16] D'Aguanno, D., Marignetti, F., Faginoli, F., & El-Shahat, A. (2018). Single-phase motors for household applications. *Electric Machines for Smart Grids Applications Design, Simulation and Control, IntechOpen*, 416-908. https://doi.org/10.5772/intechopen.79203
[17] Akbaba, M. & Fakhro, S. Q. (1992). Field distribution and iron loss computation in reluctance augmented shaded-pole motors using finite element method. *IEEE Transactions on Energy Conversion, 7*(2), 302-307. https://doi.org/10.1109/60.136225
[18] Bal, G. (2011). *Special Electrical Machines*. 3th Edition, Seçkin Publications. (In Turkish).
[19] Hajek, V., Mach, M., & Kuchar, L. (2015, September). Special small electric motors. *International Conference on Electrical Drives and Power Electronics (EDPE)*, 296-300. https://doi.org/10.1109/EDPE.2015.7325309
[20] Dalcalı, A. & Akbaba, M. (2017). FEM Study of the Effects of Geometric Changes on the Variable Reluctance Shaded-Pole Motors Performance. *The 6th Paris International Conference on Recent Trends in Engineering and Technology*.
[21] Murthy, K. V. (2008). Computer-aided design of electrical machines (pp. 223-276). Hyderabad, India: BS Publications.
[22] Akbaba, M. (1984). A Study on Shaded-Pole Induction Motors with Variable Air Gap. Associate Professorship Thesis, Karadeniz Technical University, Trabzon, Turkey.
[23] Brush, E. F., Cowie, J. G., Peters, D. T., & Son, D. J. V. (2003). Die-cast copper motor rotors: motor test results, copper compared to aluminium. *Energy efficiency in motor driven SYSTEMS*, Springer, Berlin, Heidelberg, 136-143. https://doi.org/10.1007/978-3-642-55475-9_21

Authors' contacts:

Adem Dalcali, Assoc. Prof. Dr.
(Corresponding author)
(1) Department of Electrical and Electronics Engineering,
Bandırma Onyedi Eylül University,
Bandırma, Balıkesir, Turkey
(2) National Research University, TIIAME,
100000, Tashkent, Uzbekistan
+902667170117, adalcali@bandirma.edu.tr

Mehmet Akbaba, Prof. Dr.
Department of Computer Engineering,
College of Engineering,
Karabük University,
Karabük, Turkey
+905332645060, mehmetakbaba2021@gmail.com